Synchrotron small angle X-ray scattering for the evaluation of silica nanotubes interaction with lipid membranes

Cláudia Nunes[1, a, §], Célia T. Sousa[2, b,§], Mariana P. Proença[2], A. Apolinário[2], José L.F.C. Lima[1], Salette Reis[1], João P. Araújo[2] and Marlene Lúcio[1]

[1]REQUIMTE, Departamento de Química, Faculdade de Farmácia, Universidade do Porto, Portugal

[2]IFIMUP and IN – Institute of Nanoscience and Nanotechnology and Dep. Física e Astronomia, Univ. Porto, Rua do Campo Alegre 687, 4169-007 Porto, Portugal

[§] These authors have contributed equally.

[a]claununes@gmail.com and [b]celiasousa@fc.up.pt

Keywords: Silica nanotubes, nanoporous alumina templates, lipid bilayers, non-steroidal anti-inflammatory drugs.

Abstract. Synchrotron X-Ray scattering measurements were used to assess the interaction of silica nanotubes (SNTs) with membrane model systems at conditions that mimic the physiological pH of healthy (pH 7.4) and pathological (pH 5.0) cellular membranes. SNT arrays were synthesized combining the sol-gel method with a porous anodic alumina (PAA) template assisted approach. The inner surfaces of SNTs were functionalized with aminopropylethoxysilane (APTES). Scanning electron microscopy (SEM) and transmission electron microscopy (TEM) were used to characterize the nanocarriers. A therapeutic anti-inflammatory drug (naproxen) was loaded in the SNTs by electrostatic interactions between the negatively charged carboxyl group of the drug and the protonated inner surface of the nanotubes.

Small angle x-ray scattering (SAXS) measurements indicate that the unloaded SNTs do not interact significantly with both membranes. The negligible membrane disordering effect demonstrated by the unloaded SNTs may correlate with a desirable lack of membrane toxicity of these nanocarriers. Furthermore, the biophysical effect on membrane structure presented similar profile at pH 5.0 for the drug (non-encapsulated) and for SNTs loaded with the drug indicating that SNTs are able to release the drug content under pathological conditions.

Introduction

Silica nanoparticles have many advantages, since they are extremely stable and their size, shape and porosity can effortlessly be controlled [1]. In addition, there is no enlargement or porosity change upon pH variation; no vulnerability to microbial attack and these particles have also shown to effectively protect entrapped molecules (enzymes, drugs, etc.) against degradation [2]. Silica-based particles are also known for their biocompatibility [3, 4] and their easy surface functionalization that allows modifying the hydroxyl groups on the surface with amines, thiols, carboxyls and methacrylate, according to the desired application [5].

Moreover, high aspect ratio inorganic nanoparticles have attracted great interest for their vast applications [6]. In particular, nanotubes offer the possibility of differential functionalization that can provide the inner voids for loading drug molecules or imaging agents and the outside surface for targeting moieties, antifouling agents or different kinds of molecules. Furthermore, since the innovation of the template assisted synthesis using porous anodic alumina (PAA), it is possible to obtain monodispersed nanotubes of nearly any material with the desired length and pore diameter just by changing the anodization conditions [7].

Nowadays, the effective disease targeting represents an enormous biomedical challenge in the treatment of inflammatory diseases and other serious illnesses, since the lack of selectivity of current therapeutic agents results in numerous severe deleterious side effects, including organ and

tissue damage [8]. This constitutes a key limitation of current therapies once that drugs must often be administered at suboptimal doses to reduce cytotoxicity. Therefore, it becomes increasingly important to develop drug delivery systems that can efficiently target based on subtle molecular alterations that distinguish specifically the inflamed or other diseased cells, from the normal ones. In this context, a controlled drug release strategy can be achieved based on the sensitivity of the nanocarrier system to the pH conditions. This strategy applied to the case of non-steroidal anti-inflammatory drugs (NSAIDs) assures that the drugs are only released at the inflamed tissues (that have pH 5.0) thus minimizing the side effects of these drugs to healthy tissues (that have a pH of 7.4). Additionally, before reaching their targets and during their body distribution, drug delivery systems must cross biological membranes. Therefore it is of utmost importance to evaluate the interaction of nanocarrier systems with membranes. The study of the interaction between nanoparticles and membranes gains deeper importance in the case of silica nanotubes (SNTs) since their use could be questioned by their capacity to insert into the lipid bilayers disrupting the biophysical integrity of the membranes. Consequently, SNTs containing NSAIDs should carry the drug to the inflammation site without considerable interaction with cellular membranes of the healthy tissues.

For the pointed reasons, the present study is focused on assessing the effect of SNTs on the membrane structure and also the pH dependent release of the incorporated NSAID (naproxen) at the inflamed acidic tissues conditions. The SNTs were produced by a template assisted method using PAA. After synthesis, the voids of the SNTs were functionalized with an aminosilane, generating an inner polycationic surface, to which a negatively charged NSAID (naproxen) was electrostatically bonded. The PAA templates as well as the SNTs, before and after functionalization, were morphologically characterized using Scanning Electron Microscopy (SEM) and Transmission Electron Microscopy (TEM). The structural information about the interaction between the SNTs (loaded and unloaded) or the naproxen with the lipid bilayers was accessed by a technique widely used in biophysical studies: small angle X-ray scattering (SAXS). Synthetic lipid bilayers of 1,2-dipalmitoyl-*sn*-glycero-3-phosphocholine (DPPC) at pH 7.4 were used as biomimetic model systems, mimicking biological healthy membranes that possess a composition rich in phosphocholine. Moreover, DPPC is an endogenous component of the joints and represents approximately 45% of the total synovial fluid lipid component [9]. Hence, lipid bilayers of DPPC at pH 5.0 mimicked the biological inflammation targets of NSAIDs.

Overall the gathered results provided insight about the SNTs cellular uptake and corroborate the preferential effect of naproxen on the membranes at pathological conditions.

Experimental

For the growth of SNTs we used PAA templates obtained by a standard two-step anodization method of high-purity (99.997%) Al foils [10]. After an electropolishing pre-treatment, the Al foils were anodized in a 0.3 M oxalic acid solution at 4 °C and under an applied potential of 40 V [11]. The first anodization was carried out for 24 h while the second lasted 15 min. These anodization conditions resulted in nanopores with an average diameter of 35 nm, separation of 105 nm, and 500 nm in length. The polymeric SNTs were prepared combining the PAA template assisted method with a sol obtained under acidic conditions using tetraethyl orthosilicate (TEOS) as a silica precursor and their inner surface were also functionalized with aminopropylethoxysilane (APTES) following a procedure described in a previous work [12].

After the inner surface functionalization with aminosilane, the PAA was dissolved and the SNTs that were inside of the PAA template were resuspended in a solution of KOH (0.1 M) for 10 min, centrifuged at 35000 G for 25 min and washed with bideionised water. Then the SNTs were again resuspended in a Hepes buffered solution (pH = 7.4) of naproxen (10 μM) and incubated in the dark for 2 h with continuous agitation. In order to wash and remove the excess of naproxen that was not attached to the inner surface of the SNTs, the suspension was again washed with bideionised water and centrifuged three times.

The size and morphology of the nanostructures were determined by Scanning Electron Microscopy (SEM) analysis in a FEI Quanta 400 FEG SEM and by Transmission Electron Microscopy (TEM) in a LEO 906E Leica.

SAXS experiments were performed at the beam line A2 of Doris III at HASYLAB (DESY, Hamburg, Germany) with a monochromatic radiation of wavelength 0.15 nm. The SAXS detector was calibrated with rat-tail tendon. Heating scans were performed at a rate of 1 °C min^{-1} in the range of 10 °C to 52 °C. Data was recorded for 10 s every minute. Static exposures were also taken below and above the main transition temperature and compared with the same temperatures at the heating cycles to check for possible radiation damage. In order to minimize the X-ray exposure to the sample, a shutter mounted before the sample was kept closed when no data was acquired. Lipid dispersions composed of multilamellar vesicles (MLVs) of DPPC mixed with naproxen, SNTs and SNTs loaded with naproxen were prepared at pH 5.0 and pH 7.4 according to a well described method [13, 14]. The SNTs lipid dispersions were prepared with a fixed concentration of $1x10^{11}$ SNTs/mL; the naproxen loaded SNTs had 162 μg of incorporated naproxen [12] and the naproxen lipid dispersions contained 30 μg/mL of drug.

Results and discussion

SNTs characterization

SNTs were easily grown inside the pores of PAA templates by combination of anodization and sol-gel techniques. Furthermore, the SNTs production method presented herein allows an accurate tailoring of the SNTs dimensions, the size homogeneity and distinct functionalization of both inner and outer walls.

Detailed imaging studies were made on SNTs in PAA template and after template removal. The studies include TEM and FE-SEM. Figure 1 (a) shows a typical FE-SEM image of PAA surface. Self-ordered arrays of uniform pores are observed with pore diameter of 40 nm and inter-pore distance of 105 nm. In Fig. 1 (b) a representative SEM image of the SNTs samples are shown, in which the tubular nanostructure is clearly visible. This indicates that a one-dimensional silica material has been prepared in the form of nanotubes. The SNTs have an outer diameter of 40 nm, replicating the used PAA pore size. This indicates that the size, shape and organized hexagonal packing of the NTs are controlled by the characteristics of the template. Further structure characterization of the SNTs was performed by TEM [Fig. 1 (c)]. The TEM image confirms the outer diameter of the SNTs (40 nm), which corresponds to the pore size of the PAA template used. The image also shows an inner diameter of about 35 nm and a wall thickness of 5 nm.

SAXS measurements

DPPC molecules spontaneously form lyotropic lamellar phases in excess water, whose structure and long-range organization are temperature dependent [14, 15]. As temperature is increased from room temperature, DPPC presents three different phases: gel phase ($L_{\beta'}$), ripple phase ($P_{\beta'}$) and liquid-crystalline phase (L_α). $L_{\beta'}$ and $P_{\beta'}$ are ordered lamellar phases with tilted acyl chains predominantly in all-*trans* conformation, and L_α is the lamellar fluid phase with disordered acyl chains due to conformational changes (*trans-gauche* isomerization) (Winter 2004). In this work, the degree of perturbation of the $L_{\beta'}$ and the L_α phases of DPPC (the most biologically relevant) by SNTs loaded with naproxen was evaluated by X-ray diffraction patterns at small angles (SAXS) yielding information on the long range bilayer organization. In order to assess the effective release of the drug in a pH dependent manner the studies were carried out with SNTs loaded with naproxen at pH 7.4 and 5.0 (pH of inflamed cells). Studies of the interaction of both naproxen and unloaded SNTs with DPPC were also performed, making clear the contribution of the SNTs in the interaction of naproxen with membranes.

Lamellar lattice constants, *d*, were calculated from the small angle Bragg reflections using equation: $s=n/d$; where *s* is the lamellar spacing and *n* the order of the reflection (n = 1, 2, …). To obtain a more precise position for *s*, the diffraction peaks were fitted with Lorentzians and the

positions of maximum intensities and full widths of peaks at one half of their intensity were determined.

The SAXS analysis of the effects of naproxen, SNTs and SNTs loaded with naproxen, towards the DPPC bilayer at pH 7.4 (Figure 2-I) shows that no significant differences are observed in the $L_{\beta'}$ phase of DPPC. The position of the Bragg peaks was not significantly affected by the presence of both the drug and the nanosystem and *d* value remains about the same as the one of pure DPPC (Table 1). However, the Bragg peaks correspondent to mixtures of lipid and SNTs loaded with naproxen show a higher full width at half maximum than the diffraction peak correspondent to pure DPPC (Figure 2-I), indicating that the correlation between the bilayers (ξ) is slightly decreased by the presence of the nanosystem, which points to a decrease in the lipid order. In fact, three peaks are deconvoluted and correspond to the contributions of the pure lipid, the lipid:naproxen, and the lipid:SNTs. At pH 5.0 and still at the $L_{\beta'}$, it is observed that naproxen alone leads to the splitting of the first-order Bragg peak (Figure 2B-II). One peak is located at a *d* value of 6.41 nm (same as pure DPPC), and the other reflection has a spacing of 7.42 nm. The coexistence of a non-influenced lipid phase and an influenced lipid phase indicates that at the tested concentration there are not enough drug molecules to reach a homogeneous distribution of the drug within the lipid membrane. The same kind of behavior can be observed for the SNTs loaded with naproxen, with the exception that in this case (Figure 2D-II) the influenced phase has a higher contribution and this can only be attributed to the fact that at this pH the electrostatic bond between the drug and the SNTs is weakened causing a release of naproxen from the SNTs. Indeed, the SNTs alone do not provoke any perturbing effect (Figure 2C-II) in the lipid structure, confirming that the effects observed for the SNTs loaded with naproxen (Figure 2D-II) must be due to the drug release from the nanotubes.

Looking to L_{α} phase (Figure 3), the addition of naproxen at pH 7.4 (Figure 3B-I) led to a slight increase of the *d* value to 7.15 nm (Table 1). Such an increase of the long spacing could be the result of a change in the hydration behavior of DPPC due to interaction with naproxen in the disordered liquid-crystalline phase. Once more, the SNTs alone have no relevant effect in the structure of the membrane, and the same is observed for the SNTs loaded with naproxen, which means that no naproxen was released from the interior of the nanotubes.

At pH 5.0, in the L_{α} phase it is possible to see that naproxen leads again to the splitting of the Bragg peaks (Figure 3B-II), which is a sign of the coexistence of a non-influenced phase and an influenced one. On the other hand, the mixture of lipid with SNTs loaded with naproxen presents only one Bragg peak with the *d* value of 8.62 nm (Figure 3D-II). This increase can be only due to the release of naproxen and to the interaction of the drug with the lipid bilayer, once the SNTs alone produced no visible effect (Figure 3C-II). The interaction observed (increase of *d* values) results in the change in the hydration behavior of DPPC, enhancing the water layer between bilayers. The much higher *d* value obtained for the interaction of lipid membranes with SNTs loaded with naproxen than for the interaction of lipid membranes with naproxen alone, resides in the fact that the naproxen loaded into the nanotubes is in higher concentration than the naproxen added alone to the lipid membrane. Therefore, upon release from the SNTs observed at this pH, naproxen is in higher concentration in the membrane in Figure 3D-II than in Figure 3B-II. Upon interaction of the loaded SNTs with the lipid membranes at pH 5.0 the phase transition temperature is dislocated to lower values (Figure 4 (A)). This indicates that naproxen released at this pH is able to reduce the phase transition temperature of the lipid membrane to 38 ºC in comparison to the 42 °C obtained in pure DPPC bilayers. Such a significant reduction of the lipid membrane phase transition temperature is consistent with a membrane fluidization effect of naproxen that is required for its therapeutic effect.

Conclusions

The SNTs pH sensitive naproxen delivery system is based on the strength of electrostatic interactions between the drug molecules and the amino groups on the inner surface of nanotubes,

which is mainly determined by the pKa value of the drug. At pH 7.4, APTES is completely positively charged, whereas naproxen (pKa 4.2) is almost completely negatively charged, establishing thereby a strong link between the two. At pH 5.0, naproxen becomes more neutral, being only partially ionized. Hence, a much weaker Coulomb interaction is established between naproxen and the protonated amino groups on the interior of SNTs, contributing considerably to a preferable drug release at pH 5.0. Indeed, at this pH, the SAXS profile is similar to the one obtained for naproxen:DPPC mixtures, confirming thereby the release of the drug from the inner voids of the nanotubes.

At pH 7.4 the SNTs loaded with naproxen produced a negligible effect in the lipid bilayers, once the drug is protected inside of the nanotubes, and it is not released in the membrane, and for this reason the drug is not able to disturb the lipid structure.

Considering the lipid phase, the effect of the nanocarrier system loaded with the drug on the L_α phase of the lipid membrane can be associated with the anti-inflammatory efficiency of this system. Actually, to be efficient, NSAIDs must pass through several cell membranes until they reach their target enzyme (COX) which has also a membrane location. According to this, it is possible to say that the SNTs loaded with naproxen are able to release the drug at the pH of the inflamed tissues being also able to interact with the L_α phase of the membrane, as required to exert the anti-inflammatory effects *in vivo*.

Moreover, and once the SNTs alone did not perturb the membrane organization properties, it can be concluded that the SNTs uptake does not involve insertion and diffusion of the nanotubes across cell membranes, as it is also described for carbon nanotubes [16].

References

1. S.J. Son, X. Baia, A. Nan, H. Ghandeharib, and S.B. Lee, Template synthesis of multifunctional nanotubes for controlled release, J. Control. Release, 114(2006) 143-152.
2. R.K. Sharma, S. Das, and A. Maitra, Enzymes in the cavity of hollow silica nanoparticles. Journal of Colloid and Interface Science,. 284(2005) 358-361.
3. S. Natsugoe, M. Shimada, T. Kumanohoso, K. Tokuda, M. Baba, H. Yoshinaka, T. Fukumoto, K. Nakamura, K. Yamada, T. Nakashima and T. Aikou, Enhanced efficacy of bleomycin adsorbed on silica particles against lymph node metastasis, 23rd International Symposium on Controlled Release of Bioactive Materials Proceedings, 940(1996) 387-388.
4. C. Barbe, J. Bartlett, L. Kong, K. Finnie, H. K. Lin, M. Larkin, S. Calleja, A. Bush and G. Calleja, Silica particles: A novel drug-delivery system, Adv. Mater., 16(2004) 1959-1966.
5. P.K. Jal, , S. Patel, and B. Mishra, Chemical modification of silica surface by immobilization of functional groups for extractive concentration of metal ions, Talanta, 62(2004) 1005-1028.
6. S.J. Son, X. Bai, and S.B. Lee, Inorganic hollow nanoparticles and nanotubes in nanomedicine. Part 1. Drug/gene delivery applications, Drug Discov. Today, 12(2007) 650-656.
7. S. Ono, M. Saito and H. Asoh, Self-ordering of anodic porous alumina formed in organic acid electrolytes, Electrochim. Acta, 51(2005) 827–833.
8. C. Hawkins and G. W. Hanks, J. Pain Sym. Manag., 20(2000) 140-144.
9. O. Jordan, N. Butoescu and E. Doelker, Intra-articular drug delivery systems for the treatment of rheumatic diseases: A review of the factors influencing their performance, Eur. J. Pharm. Biopharm, 73 (2009) 205-218.

10. H. Masuda, and K. Fukuda. Ordered Metal Nanohole Arrays Made by a 2-Step Replication of Honeycomb Structures of Anodic Alumina, Science, 268(1995) 1466-1468.
11. D. C. Leitao, A. Apolinário, C. T. Sousa, M. Vazquez, J. B. Sousa and J. P. Araújo. Influence of the aluminum surface roughness on the porous structure of nanoporous alumina templates, J. Phys. Chem. C, 115 (2011) 8567.
12. C. T. Sousa, C. Nunes, M. P. Proença, D. C. Leitão, J. L. F. C. Lima, S. Reis, J. P. Araújo and M. Lúcio.pH sensitive silica nanotubes as rationally designed vehicles for NSAIDs delivery. Submitted to Journal of Colloids and Interfacial Science (2011).
13. C. Nunes, G. Brezesinski, J.L.F.C. Lima, S. Reis, and M. Lucio, Synchrotron SAXS and WAXS Study of the Interactions of NSAIDs with Lipid Membranes, J. Phys. Chem. B 115(2011) 8024-8032.
14. C. Nunes, G. Brezesinski, J.L.F.C. Lima, S. Reis, and M. Lucio, Effects of non-steroidal anti-inflammatory drugs on the structure of lipid bilayers: therapeutical aspects, Soft Matter 7(2011) 3002-3010.
15. B. Pili, C. Bourgaux , H. Amenitsch , G. Keller , S. Lepêtre-Mouelhi , D. Desmaële , P. Couvreur , M. Ollivon , Interaction of a new anticancer prodrug, gemcitabine-squalene, with a model membrane Coupled DSC and XRD study, Biochim. Biophys. Acta - Biomembranes 1798(2010) 1522-1532.
16. N.W.S. Kam, Z. Liu, and H. Dai, Carbon nanotubes as intracellular transporters for proteins and DNA: An investigation of the uptake mechanism and pathway, Angew. Chem Int. Edit., 45(2006) 577-581.

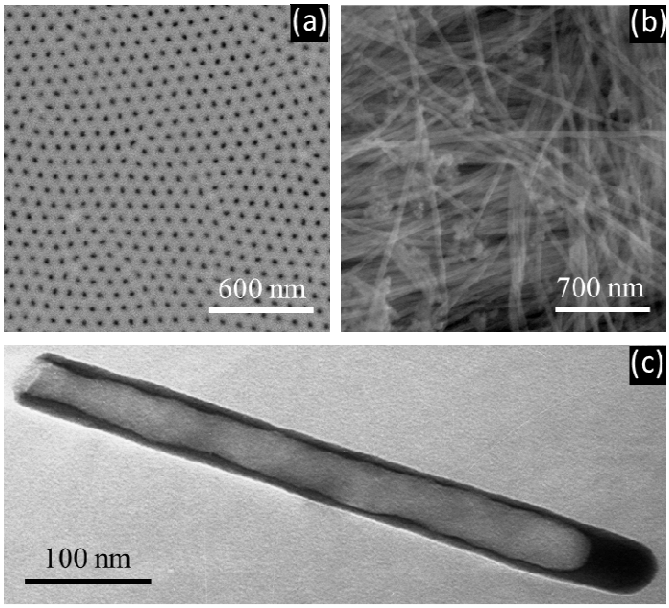

Figure 1. (a) Surface FE-SEM of a PAA template; FE-SEM image of SNTs after complete removal of PAA template and (c) TEM image of an isolated SNT.

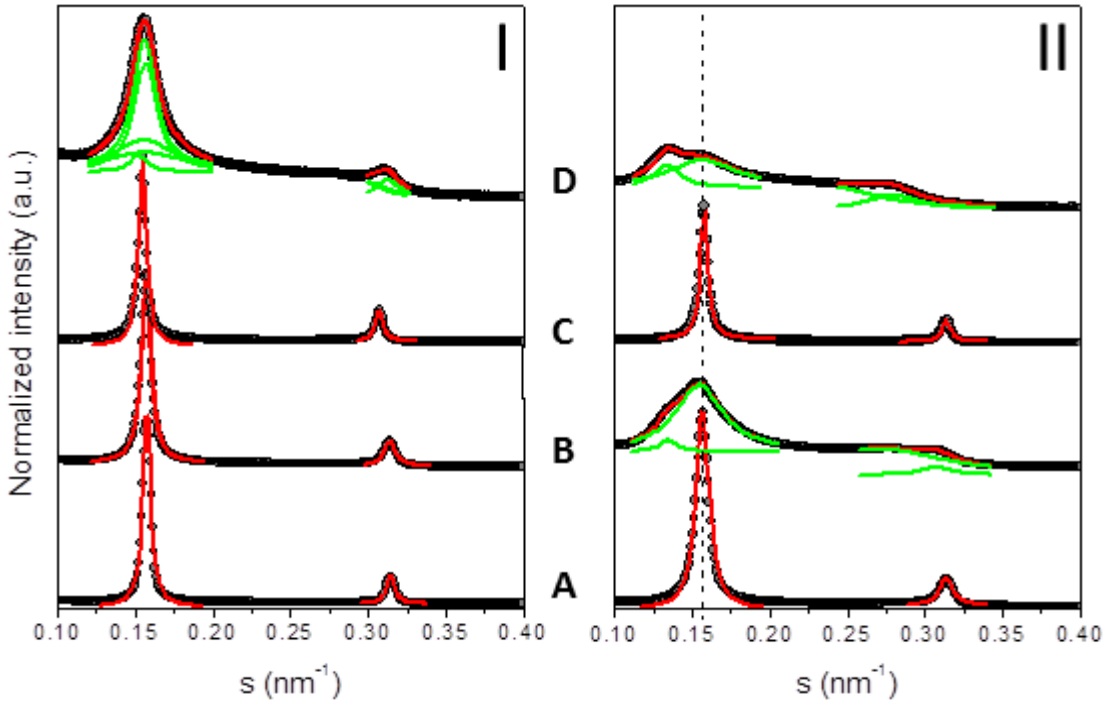

Figure 2. Small angle X-ray diffraction patterns (SAXS) at the $L_{\beta'}$ phase for DPPC (A) and subsequent mixtures with naproxen (B), silica nanotubes (C) and silica nanotubes loaded with naproxen (D) at pH 7.4 (I) and pH 5.0 (II). Green lines represent the peaks deconvolution and red lines give the best fit of the Lorentzian's analysis model to the scattered intensities.

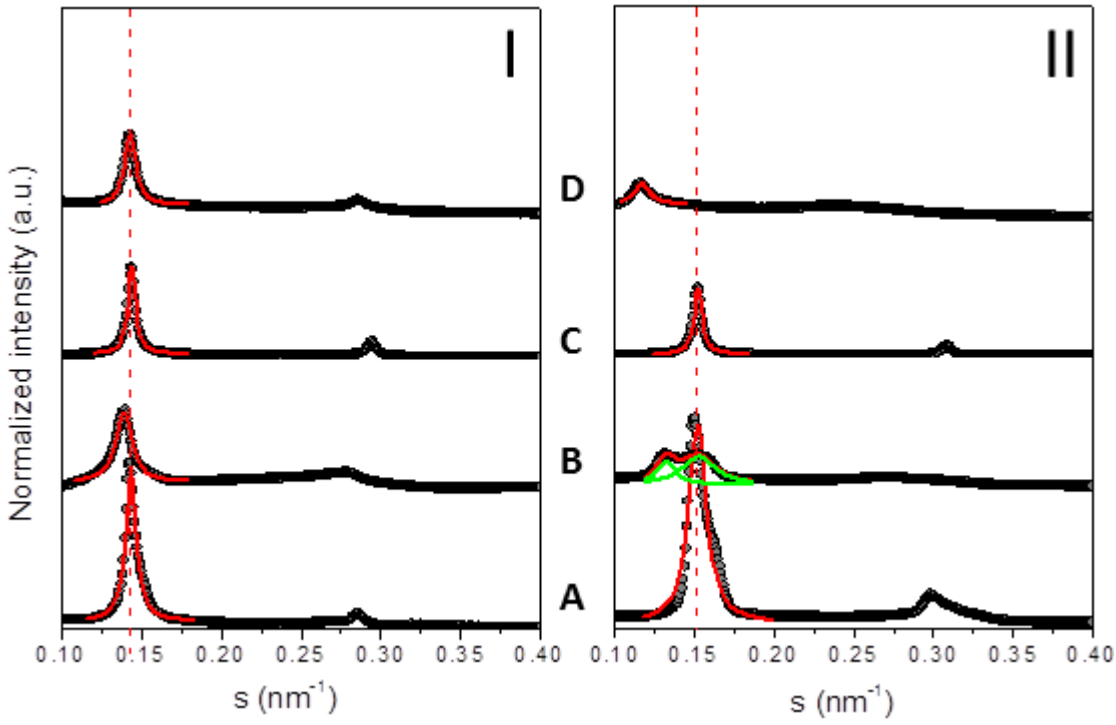

Figure 3. Small angle X-ray diffraction patterns (SAXS) at the L_{α} phase for DPPC (A) and subsequent mixtures with naproxen (B), silica nanotubes (C) and silica nanotubes with incorporated naproxen (D) at pH 7.4 (I) and pH 5.0 (II). Green lines represent the peaks deconvolution and red lines give the best fit of the Lorentzian's analysis model to the scattered intensities.

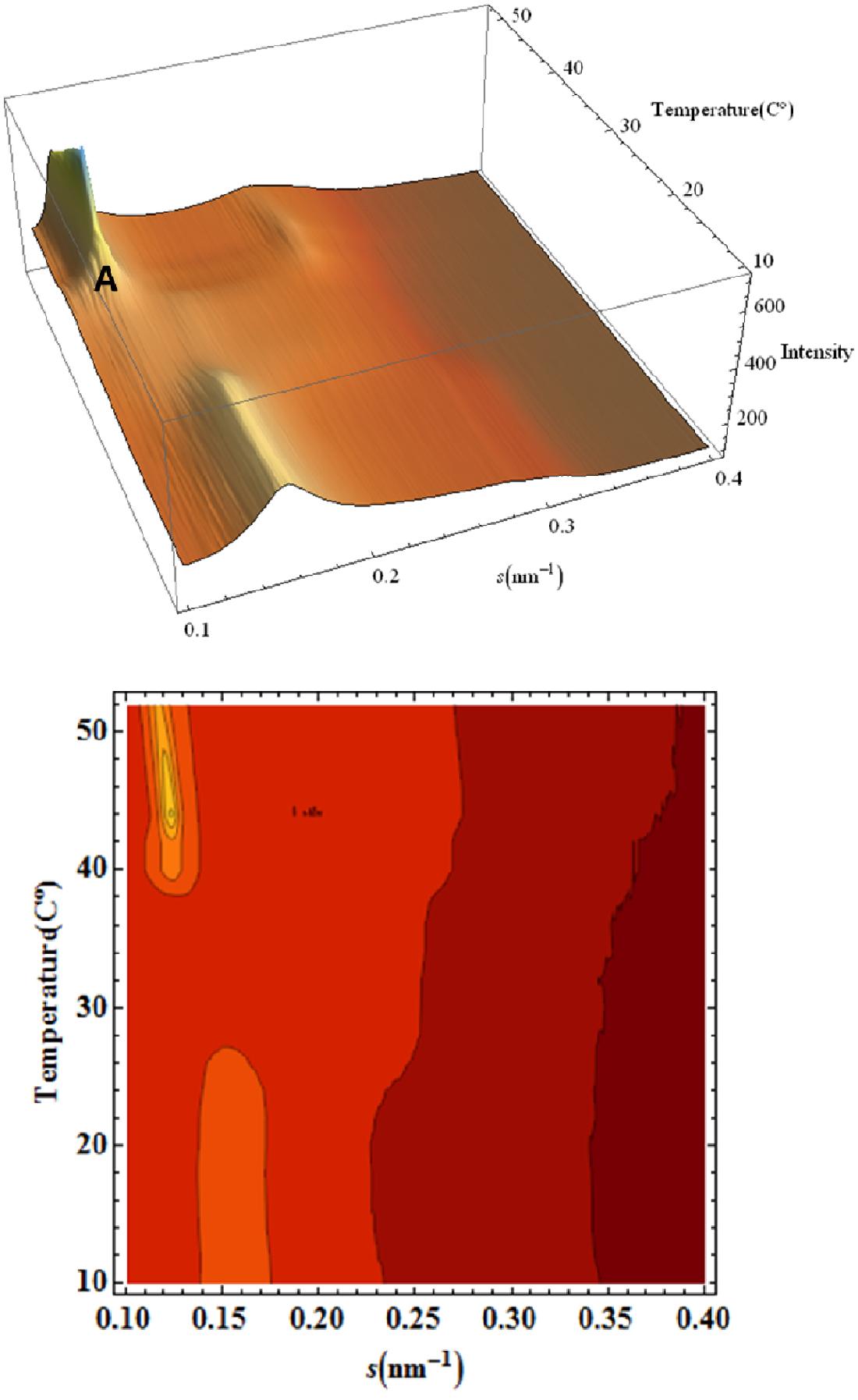

Figure 4. Three-dimensional plot of a surface representing small angle X-ray diffraction (SAXS) heating scan from 10-52 °C for the DPPC mixture with SNTs loaded with naproxen at pH 5.0.

Table 1 - Long distance (*d*) and correlation length (ξ) determined from SAXS diffraction patterns, at 20 °C and 50 °C and at pH 5.0 and 7.4, respectively,

	pH	20 ° C ($L_{\beta'}$)		50 °C (L_{α})	
		d (Å)	ξ (Å)	d (Å)	ξ (Å)
DPPC	5.0	65.4 ± 0.5	116 ± 10	65.8 ± 0.5	120 ± 10
	7.4	63.8 ± 0.5	157 ± 10	69.7 ± 0.5	131 ± 10
DPPC + naproxen	5.0	74.5 ± 0.5	69 ± 10	73.6 ± 0.5	62 ± 10
	7.4	63.7 ± 0.5	133 ± 10	71.9 ± 0.5	136 ± 10
DPPC+SNTs	5.0	65 ± 0.5	98 ± 10	65.6 ± 0.5	127 ± 10
	7.4	64.2 ± 0.5	123 ± 10	69.4 ± 0.5	170 ± 10
DPPC + naproxen loaded SNTs	5.0	79.9 ± 0.5	49 ± 10	85.4 ± 0.5	86 ± 10
	7.4	64.2 ± 0.5	87 ± 10	66.2 ± 0.5	65 ± 10